ESTIMATION OF THE ATTENUATION AND DIFFUSION FUNCTIONS IN PLASTIC OPTICAL FIBERS FROM EXPERIMENTAL FAR FIELD PATTERNS

M. Ángeles Losada [1], Javier Mateo [1], Ignacio Garcés [1], Joseba Zubia [2]

[1] I3A Universidad de Zaragoza, C María de Luna 1, Zaragoza 50018, Spain.

alosada@unizar.es, jmateo@unizar.es, ngarces@unizar.es

[2] ETSII y de IT, Universidad del Pais Vasco, Alameda de Urquijo sn, 48013 Bilbao, Spain.

jtpzuzaj@bi.ehu.es

Abstract

We have characterized step-index plastic optical fibers (SI-POFs) by estimating generalized diffusion and attenuation functions of the propagation angle. We assume that power flow is described by Gloge´s differential equation and find a global solution that was fitted to experimental far field patterns (FFPs) registered using a CCD camera as a function of fiber length. The diffusion and attenuation functions obtained describe completely the fiber behavior and can be used along with the power flow equation to predict the optical power distribution for any launching condition and for any fiber length. Using this approach, we simulate the experimental procedure proposed to estimate the coupling strength based on the changes in the fiber output power pattern in order to analyze its performance.

1. Introduction

The shape of the FFP of a POF is determined by the angular distribution of optical power at the output of the fiber that depends on the initial distribution given by the launching condition, on power diffusion and attenuation and, naturally, on fiber length. Gloge's equation has been frequently used to describe the evolution of the modal power distribution with fiber length [1], although most previous works assumed several approximations that are not consistent with some features found in experimental FFPs. Therefore, we propose a model where diffusion and attenuation are described by functions of the propagation angle showing that a constant diffusion predicts our experimental FFPs with less accuracy than a more general diffusion function. We characterize three SI-POFs from different manufactures by obtaining their diffusion and attenuation functions that can be introduced in Gloge's differential equation to solve it using different initial distributions. As we have found that constant diffusion does not give a good description of the behavior of high NA POFs, we want to analyze how this affects the experimental method proposed by Gambling el al. [2] to measure the coupling strength (here called diffusion constant) which is based, naturally, on the assumption that diffusion can be accurately modeled by a constant value. Our aim is to simulate the experimental

procedure and to compare the predictions of our model using both constant and sigmoid diffusion functions to verify which reproduces better previous experimental findings.

The paper is organized as follows. We first give a brief overview of our model and then, describe the experimental method to obtain FFPs as a function of fiber length and how these measurements are used to characterize the POFs [3]. In the third section, we describe the simulation of Gambling method which is based on launching a plane wave at different angles onto the fiber to determine the transition angle for which the fiber output pattern changes from a disk to a ring. In the last section, we summarize the conclusions drawn from our results.

2. Fiber propagation model

We propose a more general model based on finding a global solution for the following equation:

$$\frac{\partial P(\theta,z)}{\partial z} = -\alpha(\theta)P(\theta,z) + \frac{1}{\theta}\frac{\partial}{\partial\theta}\left(\theta D(\theta)\frac{\partial P(\theta,z)}{\partial\theta}\right) \quad (1)$$

where both fiber diffusion $D(\theta)$ and attenuation $\alpha(\theta)$ are described by angular functions of the inner propagation angle. For large z values, when the angular power distribution has reached its steady state distribution (SSD), the solution of the equation can be expressed as the product of two functions of independent variables: $P_{SSD} = Q(\theta)e^{-\gamma z}$ where $Q(\theta)$ describes the shape of the SSD profile, while the dependence on fiber length z is given by a decreasing exponential function which accounts for the power decrease due to the fiber attenuation γ. Introducing P_{SSD} into Eq. (1), gives an expression of $\alpha(\theta)$ in terms of $D(\theta)$ and $Q(\theta)$ as follows:

$$\alpha(\theta) = \gamma + \frac{1}{Q(\theta)\theta}\frac{\partial}{\partial\theta}\left[\theta D(\theta)\frac{\partial Q(\theta)}{\partial\theta}\right] \quad (2)$$

In this way, a shape for the attenuation function does not have to be assumed as it can be directly calculated. On the other hand, although fiber diffusion has usually been modeled by a constant value in POFs [4-5], we use a sigmoid function of the squared inner propagation angle given by:

$$D(\theta) = D_0 + \frac{D_1}{1 + D_2 e^{\sigma_d^2\theta^2}} \quad (3)$$

3. Fiber characterization method

In this section, we describe the experimental method to acquire the FFP images and the general procedure used to characterize the fibers by obtaining their attenuation and diffusion functions.

3.1 Experimental technique to acquire FFPs

Three high NA polymethyl methacrylate (PMMA) fibers of 1mm diameter from different manufacturers were tested: ESKA-PREMIER GH4001 (GH) from Mitsubishi, HFBR-RUS100 (HFB) from Agilent, and PGU-FB1000 (PGU) from Toray. All fibers have nominal NA near 0.5 corresponding to an inner critical angle around 19º. We used a 12 bit monochrome cooled camera QICAM FAST 1394 to register the FFP images reflected on a white screen placed opposite the fiber

output end as a function of fiber length. The input end of the fiber was connected to a transmitter based on an AlGaInP laser diode (LD SANYO DL-3147-021) emitting 5mW at 645nm and with a typical divergence of 30º in the perpendicular plane, and of 7.5º in the parallel plane. The experimental procedure was the following: We started with the whole length of the fiber to test rolled onto an 18cm diameter reel and the FFP image was taken. Then, a segment of 10m/5m/2.5m was cut from the output end of the fiber and the whole procedure started again, up to 10m. The longest measured length was different for each fiber: 175m for the GH fiber, 100m for the HFB and 150m for the PGU. Further details of the method to obtain the FFPs were explained elsewhere [6].

3.2 Characterization procedure

To estimate the diffusion and attenuation functions we followed two different approaches modeling diffusion first by a constant as has been usually assumed [1,2, 4-5] and then, by the sigmoid given by Eq. (3), in order to learn which model gives predictions closer to the experimental data. Eq. (2) gives the attenuation provided γ, $Q(\theta)$ and $D(\theta)$ are known. Thus, we first estimated γ directly from our experimental data and fitted the experimental SSDs by a sigmoid-like function of the squared propagation angle to obtain an analytical form of $Q(\theta)$ and its derivatives [3]. Then, we solved numerically Eq. (1) [7] to obtain the model predictions for the FFP profiles starting with a guess for $D(\theta)$. The final estimate is the one that minimizes the RMSE between the measured FFPs and the model predictions and was found using a direct search pattern method [8]. In each iteration, the latest estimate of $D(\theta)$ was introduced in Eq. (2) to calculate the corresponding attenuation function.

In Table 1, the values of the parameters of the diffusion function for the two approaches and their corresponding RMSEs are shown. The greater RMSE values obtained for all fibers with the constant diffusion model suggest that the experimental FFPs are better described characterizing diffusion by a sigmoid function.

Table 1. Parameters for the constant diffusion and sigmoid diffusion functions that minimizes the error between experimental and model-predicted far field profiles.

	D_c		$D(\theta)$ [a]				
Fiber	Rad^2/m	*RMSE*	D_0	D_1	D_2	σ_d	*RMSE*
GH	$1.317\ 10^{-4}$	$26.5\ 10^{-3}$	$5.089\ 10^{-5}$	$10.16\ 10^{-4}$	1.78	10.32	$11.3\ 10^{-3}$
HFB	$2.045\ 10^{-4}$	$23.5\ 10^{-3}$	$5.164\ 10^{-5}$	$30.26\ 10^{-4}$	1.73	9.19	$11.0\ 10^{-3}$
PGU	$2.00\ 10^{-4}$	$27.0\ 10^{-3}$	$12.06\ 10^{-5}$	$3.035\ 10^{-4}$	0.18	12.57	$18.8\ 10^{-3}$

[a] Defined in Eq. (3).

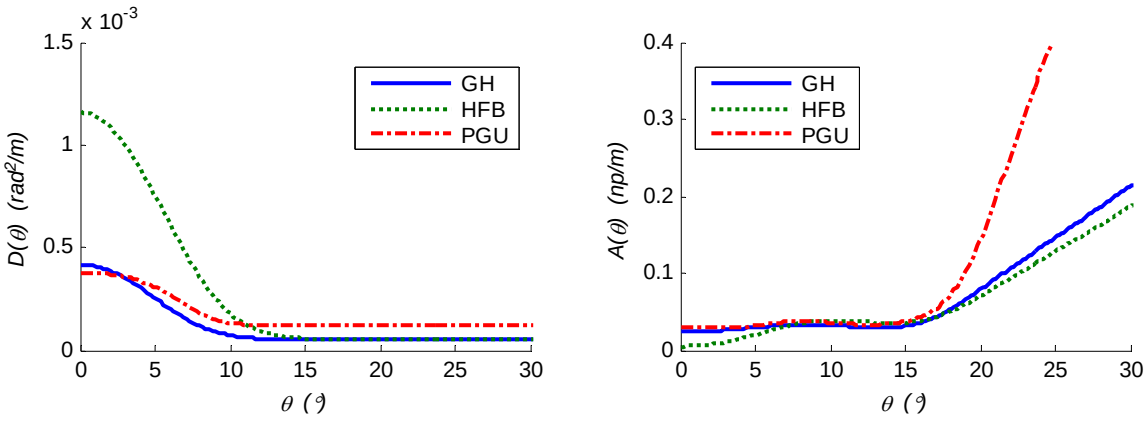

(a) Diffusion functions

(b) Attenuation functions

Fig. 1. Diffusion and attenuation functions for the three fibers obtained by modeling diffusion with the sigmoid function given by Eq. (3).

The sigmoid diffusion functions calculated introducing parameters from Table 1 into Eq. (3), and their corresponding attenuation functions obtained directly from Eq. (2) are plotted in Fig. 1 (a) and Fig. 1 (b) respectively, for the three fibers. Fig. 1 (a) displays higher diffusion at small angles, which is the dominant factor at short fiber lengths. At longer fiber lengths, however, angular attenuation has more importance, determining the shape of the SSD. Fig 1 (b) shows that attenuation is relatively flat at the lower angles and rise steeply near the critical angle although the increase is less abrupt than that postulated in other works [4-5] where it is described by a function whose value is infinity just above the critical angle. These models cannot reproduce the presence of power above the critical angle which was found in experimental patterns indicating that light paths exist beyond the critical angle.

4. Determination of the transition angle versus fiber length

Here, we analyze the experimental technique proposed in [2], where an analytical solution for Gloge's differential equation was found when the input distributions are plane waves at different angles respect to fiber axis under certain assumptions: Constant diffusion, parabolic attenuation and no upper bound for the propagation angle. From this analytical solution, the transition angle θ_t, defined as the launching angle for which the output pattern changes from a disk to a ring, can be calculated as a function of fiber length. A linear relationship in log-log coordinates for the transition angle versus fiber length can be derived using certain approximations that restrict their validity to relatively short lengths and small angles, and is given by:

$$\log(\theta_t) = 0.5\log(z) + \log\left(2D^{0.5}\right) \tag{4}$$

Thus, a method to estimate *D* that has been widely used consists in the measurement of the transition angle as a function of length and the fit of a straight line to these data to calculate *D* from the vertical intercept [9-11]. Here, we solve Gloge's differential equation introducing plane waves at

different angles as the initial power distributions, and modeling diffusion both with the constant and with the sigmoid functions defined by the parameters given in Table 1. The transition angles obtained from the simulated FFPs at each fiber length are shown in Fig. 2 for the three fibers as circles for the sigmoid function and squares for the constant function which are all fitted by straight lines (solid lines for the sigmoid diffusion model and dashed lines for the constant diffusion model). The parameters for the fits to the data simulated with the sigmoid diffusion model are given in the caption of Fig. 2. For the constant diffusion model, the fitted slopes are 0.5 and the estimated diffusion constants coincide with the value of D_c from Table 1, which confirms the validity of the experimental technique if diffusion could be described by a constant. These values of diffusion are, however, significantly smaller to those obtained experimentally in previous works by launching light from a He-Ne laser at different angles: 9.8 10^{-4} rad^2/m for the HFB fiber, and 3.5 10^{-4} rad^2/m for the GH fiber [11].

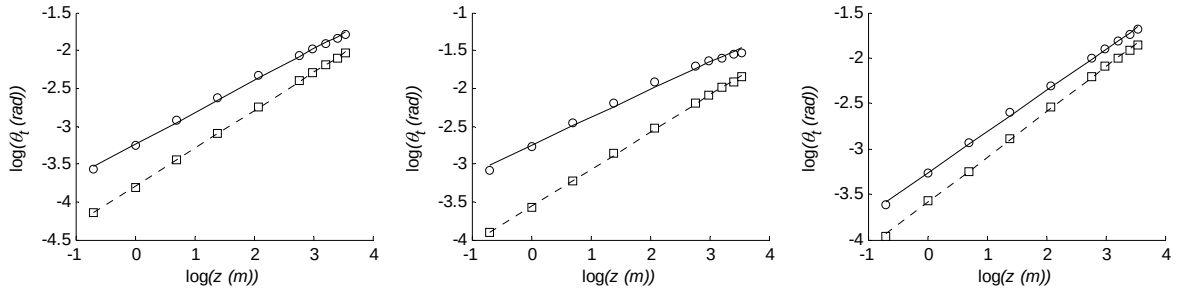

(a) GH fiber (b) HFB fiber (c) PGU fiber

Fig. 2. Transition angle versus fiber length obtained by modeling diffusion as a sigmoid function (circles for simulated data and solid lines for linear fits) and modeling as a constant (squares for simulated data and dashed lines for liner fits) for the three fibers tested. The parameters for the linear fits to the data obtained for the sigmoid diffusion model are: D=3.8 10^{-4} rad^2/m, slope: 0.42 for GH, D=10.2 10^{-4} rad^2/m, slope:0.36 for HFB, and D=3.6 10^{-4} rad^2/m slope: 0.45 for PGU.

On the other hand, the plots of the transition angle versus length predicted with sigmoid diffusion display greater deviations from linearity and the fitted slopes are always shallower than 0.5. Figures also show how the transition angles obtained using the sigmoid diffusion model are significantly higher. Consequently, the diffusion constant estimated by the linear fit of Eq. (4) to these simulated data is always higher and closer to the experimental findings. Also notice that these estimates are always between the maximum and minimum values of $D(\theta)$, but much closer to the maximum, suggesting that the main factor behind the power spread that smoothes the ring pattern towards a disk pattern is the value of the weighted average of the diffusion function at lower angles where most optical propagating power is confined.

Our results support a model of fiber diffusion with a more general function of the propagation angle, although the experimental estimates using Gambling method are a reasonable approach to the power averaged fiber diffusion.

5. Conclusions

In summary, we have characterized three high NA PMMA SI-POFs using experimental FFPs and a model based on Gloge's equation to obtain the angular diffusion and attenuation functions. We found that FFPs are better predicted using a sigmoid rather than a constant diffusion function. The simulation of Gambling experiment to estimate diffusion and its comparison with experimental results provide further evidence supporting a non-constant diffusion function.

Acknowledgements

This research was supported by the Comisión Interministerial de Ciencia y Tecnología (CICYT) under grant TIC2003-08361.

References

[1] Gloge, D., "Optical Power Flow in Multimode Fibers", B.S.T.J. 51, 1767-1783 (1972).

[2] Gambling, W.A., Payne, D.N., and Matsumura, H., "Mode Conversion Coefficients in Optical Fibers", Appl. Opt. 15 n. 7, 1538-1542 (1975).

[3] Mateo, J., Losada, M.A., Garcés, I., Zubia, J., "Global characterization of optical power propagation in step-index plastic optical fibers", submitted to Optical Express in May 2006.

[4] Rousseau, M. and Jeunhomme, L., "Numerical Solution of the Coupled-Power Equation in Step-Index Optical Fibers", IEEE Trans. In Microwave Theory and Techniques, MIT-25, 577-585 (1977).

[5] Djordjevich, A. and Savovic, S., "Numerical Solution of the Power Flow Equation in Step-Index Plastic Optical Fibers", J. Opt. Soc. Am. B 21, n. 8, 1437-1438 (2004).

[6] Losada, M.A., Mateo, J., Espinosa, D., Garcés, I. and Zubia, J., "Characterisation of the far field pattern for plastic optical fibres", in Procceedings of the International Conference on Plastic Optic Fibres and Application, XIII ed. (Nuremberg, Germany 2004), pp. 458-465.

[7] Skeel, R.D. and Berzins, M., "A Method for the Spatial Discretization of Parabolic Equations in One Space Variable," SIAM J. Sci. Stat. Comp. 11, 1-32 (1990).

[8] Lewis, R.M. and Torczon, V., "Pattern Search Algorithms for Bound Constrained Minimization," SIAM J. on Optimization, 9, n. 4, 1082-1099 (1999).

[9] Jiang, G., Shi, R.F., and Garito, A.F., "Mode Coupling and Equilibrium More Distribution Conditions in Plastic Optical Fibers", IEEE Phot. Tech. Lett. 9, n. 8, 1128-1130 (1997).

[10] Losada, M.A., Garcés, I., Mateo, J., Salinas, I., Lou, J. and Zubía, J., "Mode coupling contribution to radiation losses in curvatures for high and low numerical aperture plastic optical fibres", J. Lightwave Technol. 20, n. 7, 1160-1164 (2002).

[11] Losada, M.A., Mateo, J., Garcés, I., Zubía, J., Casao, J.A., and Pérez-Vela, P., "Analysis of strained plastic optical fibres", IEEE Phot. Tech. Lett. 16, n. 6, 1513-1515 (2004).